

Investigation of the Influence of Variations in Thickness and Concentration on the Optoelectronic Characteristics of p-CuI/n-InSe Photodetector

Naeemah A. Aswad and Ayed N. Saleh*

Physics Department, College of Education for Pure Science, University of Tikrit, Tikrit, 34001, Iraq

*Corresponding Author: A. N. Saleh. Email: ayed.ns@tu.edu.iq

Received: 27 October 2025; Accepted: 6 December 2025

ABSTRACT: The SCAPS-1D software was used to simulate a p-CuI/n-InSe photodetector at 300 K with AM1.5G light. The simulation results showed that, with a quantum efficiency of 97.6% at 800 nm and a responsivity of 0.67 A/W, the ideal absorber layer thickness of 0.8 μ m produced the highest overall performance. The specific detectivity was enhanced to 2.5×10^{15} cm·Hz $^{1/2}$ ·W $^{-3}$ and the dark current was decreased by increasing the InSe carrier concentration from 1×10^{15} cm $^{-3}$ to 3×10^{15} cm $^{-3}$. These findings show that the CuI/InSe heterojunction's broadband response, strong responsivity, and low dark current make it a viable option for near-infrared photodetection applications.

KEYWORDS: p-CuI/n-InSe heterojunction; SCAPS-1D simulation; photodetector; optoelectronic properties; absorber thickness

1 Introduction

Semiconductor p-n junction-based photodetectors are one of the most important parts of current photonic systems like optical communication, environmental tracking, and imaging technologies because they are so good at turning light into electrical messages [1,2]. In recent years, material science has worked on making the absorber and window layers better so that they have higher responsivity, quantum efficiency, and spectrum selection [3].

A group III–VI stacked semiconductor called indium selenide (InSe) has gotten a lot of attention in this field because it absorbs light very well in the visible and near-infrared (NIR) ranges, electrons move quickly, and its straight bandgap energy is about 1.25 eV [4]. Because of these features, InSe is a potentially useful n-type absorber material for detecting a wide range of light.

On the other hand, copper(I) iodide (CuI), a p-type semiconductor, has a wide bandgap (\approx 3.1 eV), a lot of hole motion, great visual clarity, and chemical stability [5]. Since these things are good, CuI is often used as a window or hole transport layer in solar and photodetector systems.

When p-CuI and n-InSe are mixed, they form a heterojunction with the right band alignment. This makes it easy for carriers to separate and move across the contact [6]. This mixed structure might be able to offer low dark current and high detectivity, especially in the near-infrared (NIR) range, where many current photodetectors don't work well.

So, this study uses the SCAPS-1D modeling tool to look into how the thickness of the absorber and the amount of doping affect the optoelectronic features of a p-CuI/n-InSe heterojunction photodetector. The construction of the device is designed for higher detectivity, quantum efficiency, and responsivity so that it can be used in advanced light and sensor applications.

2 Simulation Method

The p–CuI/n–InSe photodetector was numerically simulated using the SCAPS-1D algorithm developed at Ghent University by Burgelman and associates [7]. SCAPS-1D is a one-dimensional simulator of solar cells and photodetectors based on the solution of Poisson's and continuity equations for electrons and holes under steady-state conditions [8].

2.1 Device Structure

The investigated device has the configuration shown in Fig. 1 below:

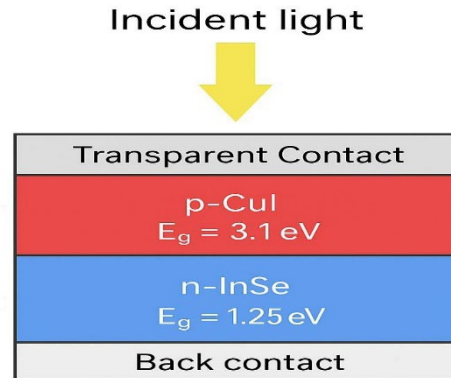


Figure 1: Shows device structure.

where ITO (Indium Tin Oxide) is the transparent front contact, CuI is the p-type window layer, InSe is the n-type absorber layer, and Ag is the back metallic contact. The design of the structure ensured high optical transparency and efficient carrier extraction across the junction.

With a bandgap of about 3.1 eV, hole mobility of $44 \text{ cm}^2/\text{V}\cdot\text{s}$, and electron affinity of 2.1 eV, the p–CuI layer provides favorable band alignment with InSe [9] and high transparency in the visible range.

Rapid electron transport and substantial light absorption are made possible by the n–InSe layer, which has a straight bandgap of 1.25 eV and an electron mobility of $600 \text{ cm}^2/\text{V}\cdot\text{s}$ [10].

In the 400–1000 nm incident wavelength region, ITO offers reduced reflection losses, while the Ag layer ensures efficient Ohmic contact with InSe.

2.2 Simulation Parameters

The simulation was conducted at 300 K with AM1.5G solar spectrum illumination (100 mW/cm^2). The applied voltage ranged from -0.8 V to 0 V , and it was assumed that the front and rear contacts were both Ohmic. Defect densities, carrier mobilities, electron affinity (χ), and bandgap energy (E_g) were among the components of the model that were borrowed from earlier theoretical and experimental investigations [3–5]. Table 1 displays the key photodetector parameters utilized in the p–CuI/n–InSe simulation.

Table 1: presents the principal fundamental detector settings inside the SCAPS simulation software.

Layers	E _g (eV)	μ _n (cm ² /v·s)	μ _p (cm ² /v·s)	N _c (cm ⁻³)	N _v (cm ⁻³)	Electron Affinity χ (V)
p-CuI [5]	3.1	100	50	2.8 × 10 ¹⁹	1 × 10 ¹⁹	2.1
InSe [3]	1.25	1000	100	1.57 × 10 ¹⁸	3.63 × 10 ¹⁹	4.7

The simulated structure enables evaluation of how the absorber thickness (0.7–0.9 μm) and donor concentration (1 × 10¹⁵–3 × 10¹⁵ cm⁻³) influence the optoelectronic response of the device. This approach provides a comprehensive understanding of the trade-off between absorption efficiency, recombination rate, and carrier transport mechanisms.

2.2.1 Spectral Response (R)

The ratio of the photocurrent (I_{ph}) generated by the photodetector to the incoming light power (P₀) at a certain wavelength (A), represented in amperes per watt (A/W), is known as the spectral response (R). By utilizing simulation tools to measure the photocurrent and light the photodetector, the spectrum response was replicated. The following Eq. (1) [6] was then used to calculate the photo response:

$$R = \frac{I_{ph}}{P_0} \quad \text{Or} \quad R = \frac{V_{ph}}{P_0} \quad (1)$$

where I_{ph} represents the photocurrent, whereas P₀ denotes the incident photoelectric power.

2.2.2 Quantum Efficiency

Quantum efficiency is defined as the ratio of the quantity of created electron-hole pairs to the quantity of incident light photons. Quantum efficiency is represented as a percentage and is determined using the subsequent Eq. (2) [7]:

$$\eta = \frac{N_{carriers}}{N_{photons}} = \frac{(I_{ph}/q)}{(P_s/hv)} \quad (2)$$

where I_{ph} is the photocurrent, q is the charge, h is Planck's constant, v is the frequency, and P_s is the photoelectric power.

2.2.3 Detectivity

It is defined as the reciprocal of the equivalent noise power or the ratio of the spectral response to the noise current, as in the following Eq. (3) [8]:

$$D = R/I_n = I/NEP \quad (3)$$

where I_n is the dark current, NEP is the noise.

The term particular detection (D*) is utilized to compare various types of photodetectors, as seen in Fig. 2. The particular detection is quantified in (cm/HZ^{1/2}·W⁻¹) and is delineated by the subsequent relationship (4) [9]:

$$D^* = \frac{(A \cdot \Delta f)^{1/2}}{NEP} = (A \cdot \Delta f)^{1/2} \cdot D \quad (4)$$

where A is the area of the photodetector, Δf is the frequency bandwidth.

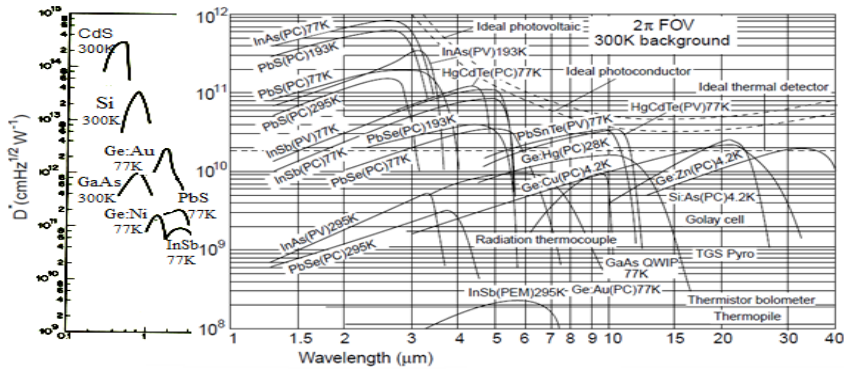


Figure 2: Specific detection D^* as a function of wavelength λ for several types of photodetectors [10].

2.2.4 Dark Current

Dark current (I_d) refers to the current that traverses a photodetector in the absence of incoming light, mostly resulting from the thermal production of charge carriers. Dark current has been modeled in the absence of illumination, as a minimal dark current is crucial for enhanced sensitivity in photo detection applications [11].

3 Results and Discussion

3.1 Influence of n-InSe Absorber Layer Thickness on p-CuI/n-InSe Photodetector Characteristics

3.1.1 Influence of Absorption Layer Thickness on Dark Current-Voltage Characteristics

The thickness of the n-InSe absorption layer was varied from $0.70\ \mu\text{m}$ to $0.90\ \mu\text{m}$, with the optimal thickness selected based on its impact on the dark state detector current. Analysis of the p-CuI/n-InSe photodetector in reverse bias, within a voltage range of $-0.8\ \text{V}$ to $0\ \text{V}$, revealed a reduction in dark current values as the thickness increased from $0.70\ \mu\text{m}$ to $0.90\ \mu\text{m}$. Furthermore, no increase in current was observed with the elevation of reverse bias voltage for the n-InSe absorption layer in the p-CuI/n-InSe photodetector, as illustrated in Fig. 3.

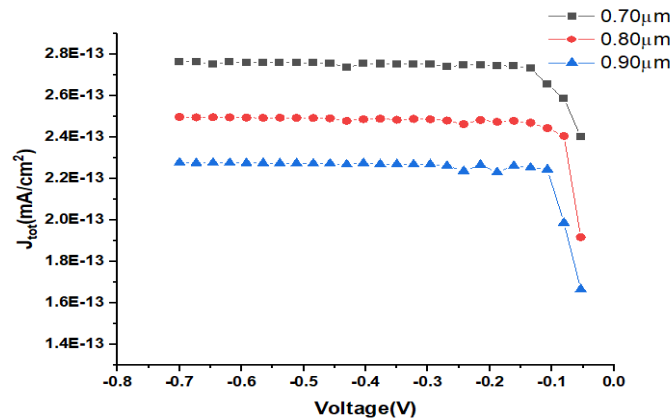


Figure 3: Current-voltage characteristics when the thickness of the absorption layer changes under reverse bias.

3.1.2 Impact of Variations in Thickness on Quantum Efficiency

Fig. 4 illustrates the quantum efficiency curves for a p-cui/n-InSe photodetector as a function of incident light wavelength, spanning from 200 nm to 1200 nm, with variations in the thickness of the n-InSe absorption layer ranging from 0.70 μm to 0.90 μm , under a reverse bias voltage of -0.5 V. The illustration depicts a progressive enhancement in quantum efficiency with the augmentation of the absorption layer's thickness within the visible and infrared spectral ranges, followed by a decline commencing at a wavelength of 980 nm. This aligns with the characteristics of a photodetector using an n-type absorption layer with an energy gap of 1.25 eV [4]. Note that the best thickness that provides the highest quantum efficiency is 0.80 μm .

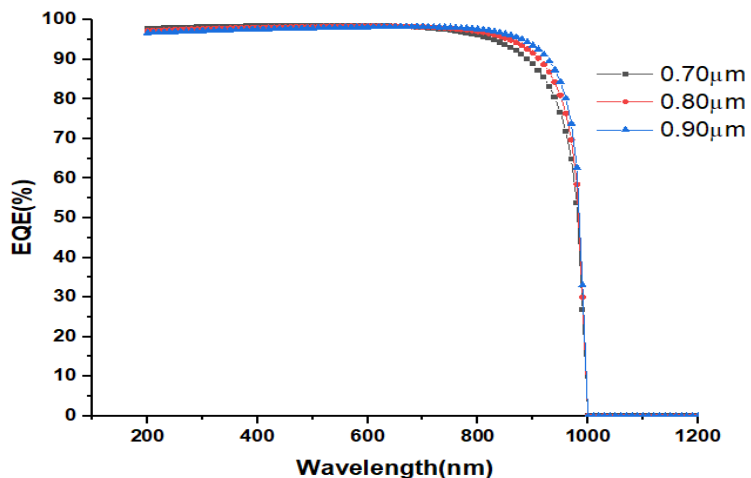


Figure 4: illustrates the variation in quantum efficiency as a function of wavelength, corresponding to alterations in the thickness of the absorption layer (n-InSe from 0.70 μm to 0.90 μm) at a reverse bias voltage of -0.5 V.

3.1.3 Impact of Varying the Thickness of the Absorption Layer on the Spectral Response

In Fig. 5, the spectral response was determined by providing an external voltage with a reverse bias of -0.5 V, which expands the depletion region and enhances the spectral response (R). The enhancement in spectrum response results from an elevated energy absorption rate, which is directly proportional to the thickness of the absorption layer, thus increasing the number of produced carriers [10,12,13]. InSe-based photodetectors demonstrate an extensive response range spanning from visible to near-infrared wavelengths, exhibiting a minor reduction in the specific detection curve at the maximum thickness of 0.90 μm for short wavelengths. Conversely, the curve at a thickness of 0.80 μm displays the optimal spectral response across all short wavelengths and near-infrared regions.

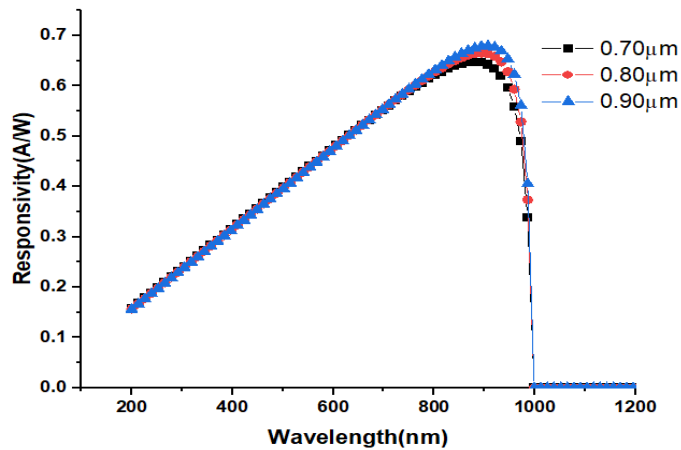


Figure 5: illustrates the spectral response as a function of wavelength, illustrating the variation in thickness of the p-CuI/n-InSe photodetector absorption layer at a reverse bias voltage of -0.5 V.

3.1.4 Impact of Varying Thickness on Particular Detection (D^*)

Fig. 6 illustrates the specific detection as a function of wavelength while varying the thickness of the InSe absorption layer from 0.70 μ m to 0.90 μ m at a reverse bias voltage of -0.5 V. The figure indicates a general rise in specific detection with the increasing thickness of the absorption layer. The increased thickness substantially absorbs light photons and creates electrons, hence enhancing the sensitivity of the photodetector. The specific detection (D^*) peaks at near-infrared wavelengths for all thicknesses, reaching its maximum at 950 nm, which corresponds to the absorption edge of the InSe material. An increase in the thickness of the n-InSe absorption layer results in a notable enhancement in specific detection, since greater thicknesses provide more photon absorption within the detectable spectral region. Absorbing photons in accordance with the energy gap results in an enhanced optical response and a reduced noise ratio, so elevating the specific detection D^* . The simulation findings indicate that regulating the thickness of the absorption layer is crucial for enhancing the photodetector's performance, particularly in the near-infrared spectrum [9,10].

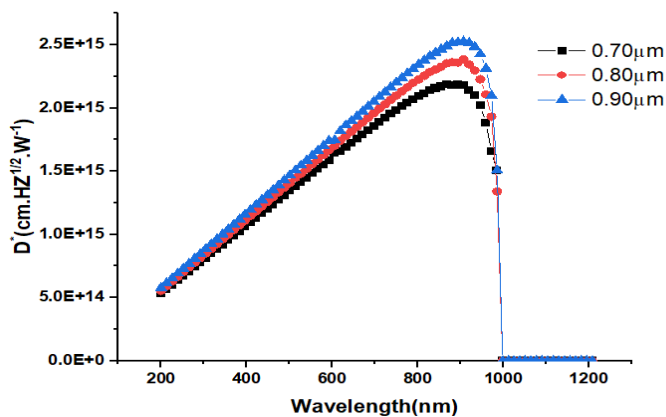


Figure 6: Specific detection as a function of wavelength with increasing thickness of the n-InSe absorption layer under reverse bias (-0.5 V).

The photodetector characteristics measured at the maximum thickness of 0.90 μ m are shown in Table 2.

Table 2: presents the recorded values of the photodetector characteristics at a thickness of 0.90 μm .

Sample	ID mA/cm^2	QE%	Responsivity (A/W)	$D^* (\text{cm} \cdot \text{Hz}^{1/2} \cdot \text{W}^{-1})$
p-CuI/ n-InSe	2.27×10^{13}	97.63%	0.675	2.525×10^{15}

3.2 Investigating the Impact of Absorption Layer Concentration

Upon determining the ideal thickness for the absorption layer (0.80 μm), we simulated the influence of varying the carrier concentration of the n-InSe absorption layer for the p-CuI/n-InSe detector, ranging from $(1 \times 10^{15} \text{--} 3 \times 10^{15}) \text{ cm}^{-3}$ at a reverse bias voltage of (-0.5 V), to assess its effect on the photodetector's performance. The doping impact of the absorption layer is contingent upon two primary factors: the kind and concentration of the impurity, as well as the material and configuration of the detector.

3.2.1 The Impact of Varying Concentration on the Current-Voltage Characteristic

Fig. 7 illustrates the impact of elevated impurity concentrations on the current-voltage curve within the range (0.7 to 0) V, under dark circumstances and at ambient temperature. An observed reduction in the current-voltage curve and a decline in the dark current value occur with an increase in carrier concentration in the absorber layer from $1 \times 10^{15} \text{ cm}^{-3}$ to $3 \times 10^{15} \text{ cm}^{-3}$.

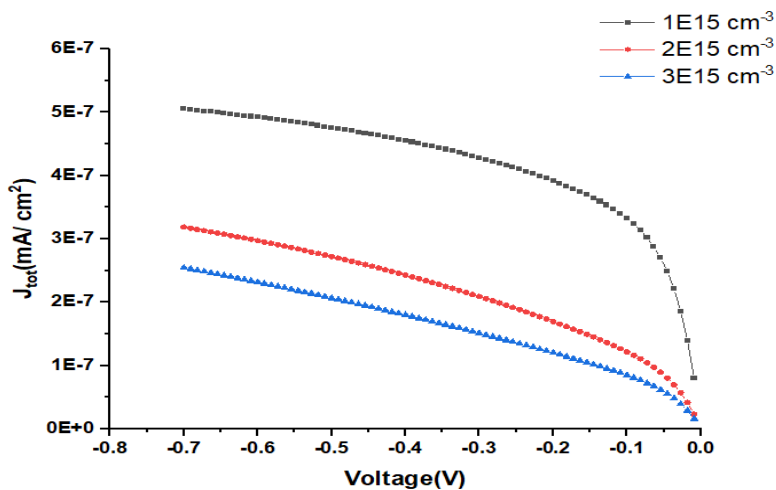


Figure 7: illustrates the impact of augmenting the concentration of the n-InSe absorption layer on the current-voltage characteristic curve.

3.2.2 Impact of Concentration Variation on Quantum Efficiency

As the carrier concentration of the n-InSe absorber layer, measuring 0.80 μm in thickness, varies from 1×10^{15} to $3 \times 10^{15} \text{ cm}^{-3}$ at a reverse bias voltage of -0.5 V in the p-CuI/n-InSe photodetector, Fig. 8, illustrates a decline in the quantum efficiency curve as a function of wavelength. The increase in carrier concentration accelerates the recombination process and diminishes the likelihood of photogenerated carriers accumulating, leading to a reduction in quantum efficiency. The overall reduction in quantum efficiency at longer wavelengths and across all concentrations arises because photons with longer wavelengths are absorbed deeper within the absorber layer, resulting in an extended diffusion length for the carriers. This extension heightens the likelihood of recombination, thereby diminishing quantum efficiency [3].

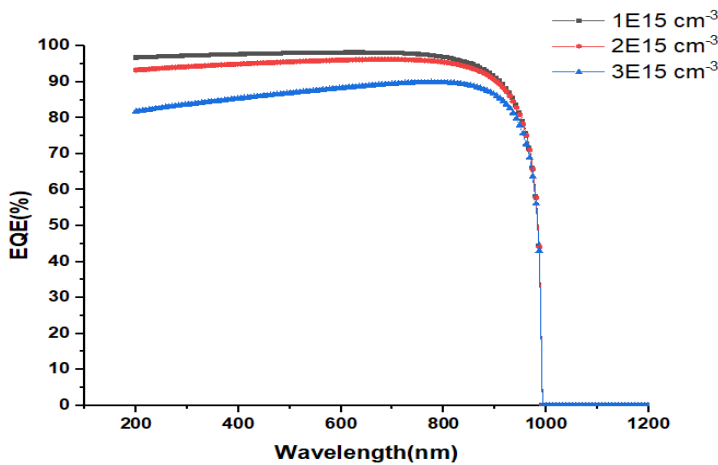


Figure 8: illustrates the correlation between quantum efficiency and concentration variation of the n-InSe absorber layer as a function of wavelength, at a reverse bias voltage of (−0.5 V).

3.2.3 Impact of Concentration Variation on Spectral Response

Fig. 9 illustrates the spectral response relative to wavelength. The variation in the concentration of the n-InSe absorber layer ranges from $1 \times 10^{15} \text{ cm}^{-3}$ to $3 \times 10^{15} \text{ cm}^{-3}$ at a reverse bias voltage of (−0.5) V. The spectral response curve rises for diminished concentrations of the n-InSe absorber layer. This results from the substantial breadth of the depletion area in the n-InSe absorber layer. When light of a certain wavelength illuminates the depletion area, it produces an external photocurrent [5,6,14].

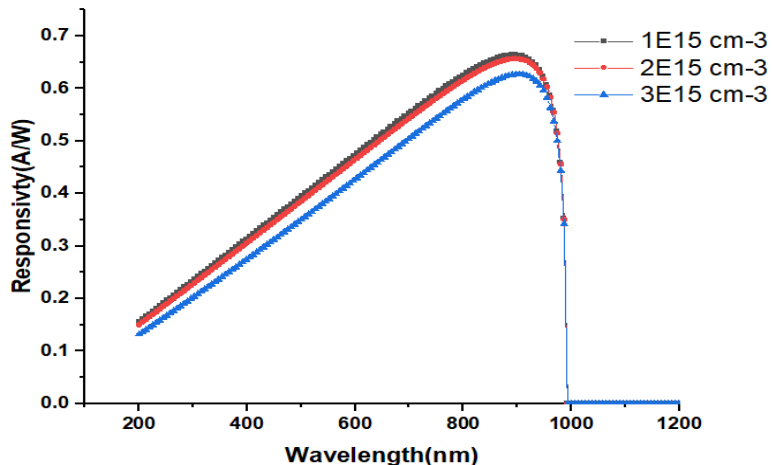


Figure 9: Spectral response as a function of wavelength with increasing impurity concentration for the n-InSe absorption layer.

3.2.4 Impact of Modifying Absorption Layer Concentration on Targeted Detection

The detector's performance, which dictates its application type and scope, may be assessed using the particular detection value (D^*). The particular detection value (D^*) is inversely correlated with the dark current; a reduction in the dark current results in an enhancement of the specific detection value. In our current simulation, and as shown in Fig. 10, at a reverse bias voltage of -0.5 V, a peak in the specific detection value is observed at long wavelengths and near-infrared radiation, which represents the absorption edge of the n-InSe absorption layer. As the wavelength exceeds 980 nm, the specific detection value diminishes due to the wavelength in this range nearing the cutoff wavelength of the n-InSe absorption layer [15].

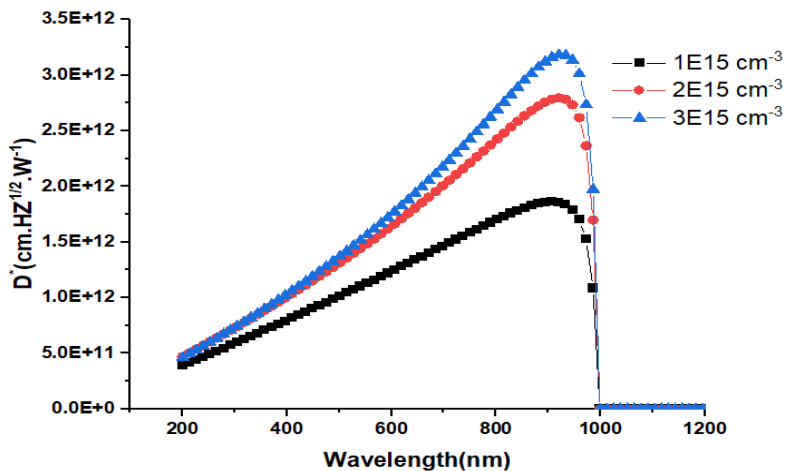


Figure 10: Specific detection as a function of wavelength while altering the concentration of the n-InSe absorption layer and at a bias voltage of (-0.5 V).

The photodetector characteristics assessed at the minimum concentration of $1 \times 10^{15} \text{ cm}^{-3}$ are likewise shown in Table 3.

Table 3: Observed values of photodetector characteristics at the maximum concentration of the n-InSe absorption layer ($3 \times 10^{15} \text{ cm}^{-3}$).

Sample	ID (mA/cm ²)	QE%	Responsivity (A/W)	D* (cm.HZ ^{1/2} .W ⁻¹)
p-CuI/n-InSe	4.75×10^{-7}	97.65	0.66	1.86×10^{12}

4 Conclusions

The simulation outcomes of the p-CuI/n-InSe photodetector utilizing the SCAPS-1D one-dimensional simulation software indicated the optimal thickness for the absorption layer to attain maximal efficiency and spectrum response. The absorption layer thickness was varied from $0.70 \mu\text{m}$ to $0.90 \mu\text{m}$ to assess optimal photodetection performance at a reverse bias voltage of -0.5 V and a temperature of 300 K. The ideal thickness was established at $0.80 \mu\text{m}$. The concentration of the n-InSe absorption layer was subsequently altered from 1×10^{15} to $3 \times 10^{15} \text{ cm}^{-3}$. The outcomes of the simulation were as follows:

The dark current value diminished as thickness increased and over the bias voltage range from -0.8 V to 0 V.

The quantum efficiency progressively improved with increasing thickness, attaining optimal efficiency at $0.80 \mu\text{m}$, reaching 97.63%. Near-infrared spectrum.

The spectral response value augmented with the thickness of the absorption layer, achieving optimal performance at a thickness of $0.80 \mu\text{m}$ and a value of 0.67 A/W.

Increasing the thickness of the n-InSe absorption layer significantly enhances selective detection, since greater thicknesses provide more photon absorption. Regulating the thickness of the absorption layer is crucial for enhancing photodetector efficacy, particularly in the near-infrared spectrum. The peak specific detection was attained at the minimal dark current of $2.5 \times 10^{15} \text{ cm} \cdot \text{Hz}^{1/2} \cdot \text{W}^{-1}$.

Simulating the influence of varying the carrier concentration of the n-InSe absorption layer in the p-CuI/n-InSe detector from (1×10^{15} to $3 \times 10^{15} \text{ cm}^{-3}$) at a reverse bias voltage of -0.5 V revealed that both quantum efficiency and spectral response values diminished with alterations in the absorption layer concentration. The particular detection reached its maximum at the greatest concentration and the lowest dark current, with a value of $1.86 \times 10^{12} \text{ cm} \cdot \text{Hz}^{1/2} \cdot \text{W}^{-1}$.

Acknowledgement: The authors would like to thank the administration of Tikrit University for their support and encouragement during this work.

Funding Statement: This research received no specific funding. The authors received no financial support for the research, authorship, or publication of this article.

Author Contributions: The authors confirm contribution to the paper as follows: The study conception, methodology design, simulation work, data collection, and primary analysis were carried out by N. A. Aswad. A. N. N. Saleh contributed to guiding the research design, supervising the analytical process, assisting in the interpretation of the results, and revising the manuscript. Both authors reviewed the findings and approved the final version of the manuscript.

Availability of Data and Materials: The data supporting the findings of this study are available from the corresponding author upon reasonable request.

Ethics Approval: Not applicable.

Conflicts of Interest: The authors declare no conflicts of interest.

References

1. Sze SM, Ng KK. Physics of semiconductor devices. Hoboken, NJ, USA: Wiley ; 2006. <http://doi.org/10.1002/0470068329>.
2. Bube RH. Photoelectronic properties of semiconductors. Cambridge, UK: Cambridge University Press; 1992.
3. Mukhopadhyay K, Mishra A, Ray S. Development of wide-bandgap heterojunction photodetectors for visible-blind applications. Mater Res Innov. 2019;23(6):402–9.
4. Li Z, Qiao H, Guo Z, Ren X, Huang Z, Qi X, et al. High-performance photo-electrochemical photodetector based on liquid-exfoliated few-layered InSe nanosheets with enhanced stability. Adv Funct Materials. 2018;28(16):1705237. <http://doi.org/10.1002/adfm.201705237>.
5. Yamada N, Ino R, Ninomiya Y. Truly transparent p-type γ -CuI thin films with high hole mobility. Chem Mater. 2016;28(14):4971–81. <http://doi.org/10.1021/acs.chemmater.6b01358>.
6. Yildiz EA. Single crystalline Holmium doped InSe for optical limiting operation in Near-IR region. Phys Scr. 2024;99(9):095941. <http://doi.org/10.1088/1402-4896/ad69ce>.
7. Burgelman M, Nollet P, Degrave S. Modelling polycrystalline semiconductor solar cells. Thin Solid Films. 2000;361:527–32. [http://doi.org/10.1016/S0040-6090\(99\)00825-1](http://doi.org/10.1016/S0040-6090(99)00825-1).
8. Burgelman M. SCAPS-1D solar cell simulation software-user's guide. Gent, Belgium: Ghent University; 2023.
9. Ren Y, An H, Zhang W, Wei S, Xing C, Peng Z. Ultrasmall SnS₂ quantum dot-based photodetectors with high responsivity and detectivity. Nanophotonics. 2022;11(21):4781–92. <http://doi.org/10.1515/nanoph-2022-0277>.
10. Luo W, Cao Y, Hu P, Cai K, Feng Q, Yan F, et al. Gate tuning of high-performance InSe-based photodetectors using graphene electrodes. Adv Opt Mater. 2015;3(10):1418–23. <http://doi.org/10.1002/adom.201500190>.
11. Seck SM, Ahmed AA, Smith J, Johnson L, Kaya M, Lee W, et al. Experimental investigation of optical properties of natural minerals for detector applications. Nat Resour. 2020;11:99–109.
12. Patil, C., Mangu, R., Krishna, S., & Hollar, C. Self-Driven Highly Responsive PN Junction InSe Heterostructure Near-Infrared Light Detector. Photonics Research, 2022.
13. Liu, S., Zhao, L., Yan, X., et al. Ultrahigh responsive negative photoconductivity photodetector based on multi-layer graphene/InSe van der Waals heterostructure. Journal of Science: Advanced Materials and Devices, 2022.
14. Kim, H., Park, J. H., Lin, H., et al. Self-powered photodetector with low dark current based on InSe/ β -Ga₂O₃ heterojunctions. Journal of Materials Chemistry C, 2024.

15. Ahmed, M., Zhou, Y., Wu, H., et al. Doping characteristics and band engineering of InSe for advanced photodetectors: a DFT study. *Nanomaterials*, 2025.